



Contents lists available at ScienceDirect

## Bioorganic &amp; Medicinal Chemistry Letters

journal homepage: [www.elsevier.com/locate/bmcl](http://www.elsevier.com/locate/bmcl)

## A potent aminonaphthalimide platinum(IV) complex with effective antitumor activities *in vitro* and *in vivo* displaying dual DNA damage effects on tumor cells

Qingpeng Wang<sup>a,\*</sup>, Yan Chen<sup>a</sup>, Guoshuai Li<sup>a,b</sup>, Yanna Zhao<sup>a</sup>, Zhifang Liu<sup>a</sup>, Ruiyan Zhang<sup>a</sup>, Min Liu<sup>a,\*</sup>, Dacheng Li<sup>a,c,\*</sup>, Jun Han<sup>a</sup>

<sup>a</sup> Institute of Biopharmaceutical Research, Liaocheng University, Liaocheng 252059, PR China

<sup>b</sup> State Key Laboratory and Institute of Elemento-Organic Chemistry, College of Chemistry, Nankai University, Tianjin 300071, PR China

<sup>c</sup> Shandong Provincial Key Laboratory of Chemical Energy Storage and Novel Cell Technology, Liaocheng University, Liaocheng 252059, PR China

## ARTICLE INFO

## Keywords:

Antitumor  
Platinum  
Prodrug  
DNA damage  
Naphthalimide

## ABSTRACT

A new aminonaphthalimide platinum(IV) complex was developed by incorporating aminonaphthalimide, a DNA intercalator, into the platinum(IV) system. This complex displayed potent antitumor activities against all tested tumor cell lines *in vitro* and showed great potential in overcoming drug resistance of cisplatin. Moreover, it remarkably inhibited the growth of CT26 xenografts in BALB/c mice without severe side effects *in vivo*. Then, the compound exhibited a dual DNA damage antitumor mechanism that it could interact with DNA in tetravalent form via the naphthalimide group to cause DNA lesion, and the further liberation of platinum(II) complex after reduction would induce remarkable secondary damage to DNA. Meanwhile, it caused cell apoptosis through an intrinsic apoptosis pathway by up-regulating the expression of caspase 3 and caspase 9.

Platinum drugs have been widely used in the chemotherapy of various types of cancers.<sup>1,2</sup> Among which, cisplatin, carboplatin and oxaliplatin display major roles in clinic. Platinum drugs cause apoptosis of cancer cells mainly through DNA damage. However, they are prone to inducing serious drug resistances and side effects, due to drug efflux, self-repair to DNA damage, and increased tolerance to DNA lesion.<sup>3,4</sup> During the past decades, abundant efforts have been devoted to enhancing activities of platinum drugs and minimizing unwanted toxic effects, and great achievements have been made in platinum drug development.<sup>5–7</sup>

Platinum(IV) complexes as versatile prodrugs of platinum(II) drugs displayed much potential in overcoming limitations of platinum(II) drugs.<sup>8–13</sup> The easily modification of the axial ligands of platinum(IV) complexes affords an effective and convenient way to construct new complexes with desired properties. The incorporation of functional moieties with potent DNA targeting properties remarkably increased the antitumor activities of the platinum(IV) complexes.<sup>14–16</sup> Complexes I and II (Fig. 1) with DNA alkylating agent chlorambucil and nucleotide excision repair inhibitor (NERi) reduced the self-repair to DNA damage of tumor cells, and enhanced their sensitivity to Pt-DNA lesions.<sup>17,18</sup> Moreover, in our previous work, the naphthalimide platinum(IV) hybrid III with dual promising DNA intercalated ligands naphthalimide

exhibited potent antitumor activities with much potential in overcoming cisplatin resistance.<sup>19,20</sup> The naphthalimide platinum(IV) compounds represent an effective antitumor scaffold possessing dual DNA damage mechanism. However, some drawbacks of complex III, such as weak water solubility, badly affected its potential application as antitumor drug. Thus, it was of great interest for us to design new complexes with enhanced solubility and bioactivities based on such naphthalimide platinum(IV) scaffold.

Herein, in continuation of our ongoing enthusiasm for the development of new antitumor agents,<sup>21–24</sup> a mono aminonaphthalimide pended platinum(IV) complex ANOxp as shown in Fig. 2 was designed, synthesized and evaluated as antitumor agent. The mono ligand modified platinum(IV) system was regarded to possess higher solubility in water than the dual substituted one, and would further exert much influence on the antitumor activities. Furthermore, oxaliplatin as the third generation of platinum(II) drug was selected as the core of platinum(IV) with the aim of gaining target compound to overcome resistance of cisplatin.<sup>25</sup> Moreover, it has been proven in our previous work that, aminonaphthalimide was a promising ligand in improving bioactivities of platinum(IV) compounds.<sup>19,20</sup> Thereby, aminonaphthalimide ligand was employed expecting that the aminonaphthalimide and platinum fragments would display synergistic DNA

\* Corresponding authors at: Institute of Biopharmaceutical Research, Liaocheng University, Liaocheng 252059, PR China (D. Li).

E-mail addresses: [lywqp@126.com](mailto:lywqp@126.com) (Q. Wang), [panpanliumin@163.com](mailto:panpanliumin@163.com) (M. Liu), [lidacheng62@163.com](mailto:lidacheng62@163.com) (D. Li).

<https://doi.org/10.1016/j.bmcl.2019.126670>

Received 21 July 2019; Received in revised form 2 September 2019; Accepted 3 September 2019

0960-894X/© 2019 Elsevier Ltd. All rights reserved.

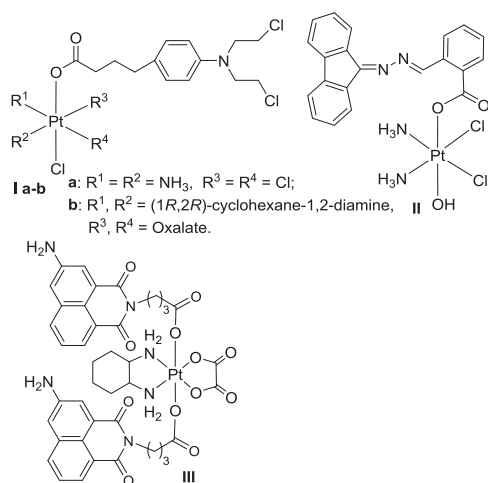


**Fig. 1.** Platinum(IV) compounds with DNA targeting axial ligands.

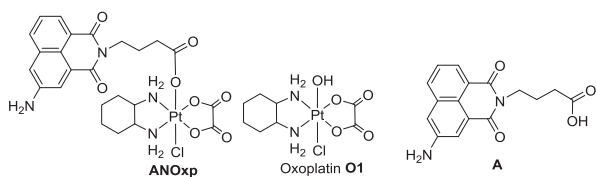


**Fig. 2.** Structures of aminonaphthalimide platinum(IV) ANOxp, oxoplatin O1 and aminonaphthalimide acid A.

damage to tumor cells. The antitumor activities *in vitro* and *in vivo* were evaluated and the potential action mechanism was also investigated.

ANOxp was prepared by the condensation of aminonaphthalimide acid A with oxoplatin O1 in yield of 24% (Fig. S1). The structure was confirmed by  $^1\text{H}$ NMR,  $^{13}\text{C}$  NMR, IR, and HRMS. The correct HRMS data of ANOxp indicates the combination of oxoplatin O1 with aminonaphthalimide acid A. Five protons upon 5.9 ppm in  $^1\text{H}$  NMR are ascribed to the protons on naphthalimide moiety. Cyclohexyl group displays peaks in upfield below 2.5 ppm. The peaks in  $^{13}\text{C}$  NMR spectrum are also appeared in the expected regions. For the IR spectrum, the carboxyl groups of ANOxp give signals in the area of  $1660\text{--}1730\text{ cm}^{-1}$ , and the aromatic frame of aminonaphthalimide fragment shows peaks between  $1623$  and  $1450\text{ cm}^{-1}$ . The purity of ANOxp is determined by HPLC (98.85%).

The antitumor activities of ANOxp against five cancer cell lines including human ovarian cancer (SKOV-3), human cervical cancer (HeLa), human lung cancer (A549), cisplatin resistant cell A549R, and murine colon cancer (CT26) were tested to evaluate its potential as antitumor agent. Moreover, the human kidney cell 293 T was used to detect its toxic properties. The results in Table 1 indicate that ANOxp could effectively inhibit the proliferation of all tested tumor cell lines with  $\text{IC}_{50}$  values below  $22.3\text{ }\mu\text{M}$ . Especially for HeLa and A549R, its

**Table 1**

Cytotoxicity profiles of complex ANOxp and oxoplatin O1 toward four human carcinoma cell lines, one murine carcinoma cell line and one normal human cell line expressed as  $\text{IC}_{50}$  ( $\mu\text{M}$ ).

Comps	SKOV-3	HeLa	A549	A549R	RF <sup>a</sup>	CT26	293 T
ANOxp	$3.8 \pm 0.4$	$2.3 \pm 0.6$	$22.3 \pm 1.2$	$10.3 \pm 0.8$	0.5	$7.1 \pm 0.9$	$6.4 \pm 0.4$
O1	$11.3 \pm 0.9$	$6.7 \pm 0.7$	$28.0 \pm 2.5$	$43.8 \pm 8.3$	1.6	$12.6 \pm 2.7$	$11.3 \pm 0.7$
A	> 100	> 100	$82.5 \pm 13.7$	> 100	NC	> 100	> 100
A&O1 <sup>b</sup>	$24.6 \pm 1.8$	$7.4 \pm 1.0$	$36.4 \pm 3.3$	$38.8 \pm 4.2$	1.1	$20.1 \pm 2.5$	$18.7 \pm 1.5$
Cisplatin	$2.4 \pm 0.2$	$2.4 \pm 0.5$	$13.5 \pm 2.1$	$22.6 \pm 3.2$	1.7	$5.3 \pm 1.9$	$12.2 \pm 0.5$
Oxaliplatin	$5.3 \pm 0.4$	$7.4 \pm 1.0$	$26.8 \pm 3.8$	$22.2 \pm 1.8$	0.8	$3.9 \pm 0.8$	$2.7 \pm 0.4$

<sup>a</sup> RF: Resistant factor.  $\text{RF}(A549) = \text{IC}_{50}(A549R)/\text{IC}_{50}(A549)$ .

<sup>b</sup> A&O1: 1 equivalent of acid A mixed with 1 equivalent of oxoplatin O1.

**Table 2**

Comparison of cytotoxicity profiles for ANOxp with complex III.

Comps	Water solubility ( $\mu\text{M}$ )	Alog P <sup>a</sup>	SKOV-3	HeLa	A549	A549R
ANOxp/Cis <sup>b</sup>	152.9	2.713	1.58	0.96	1.65	0.46
ANOxp/Oxp <sup>b</sup>			0.72	0.31	0.83	0.46
III/Cis <sup>c</sup>	37.9	3.764	2.44	4.03	2.25	0.40
III/Oxp <sup>c</sup>			1.13	1.15	1.82	0.75

<sup>a</sup> The values of Alog P were predicted by Discovery Studio.

<sup>b</sup>  $\text{ANOxp/Cis} = \text{IC}_{50}(\text{ANOxp})/\text{IC}_{50}(\text{Cisplatin})$ ;  $\text{ANOxp/Oxp} = \text{IC}_{50}(\text{ANOxp})/\text{IC}_{50}(\text{Oxaliplatin})$ . ANOxp/Cis and ANOxp/Oxp were calculated based on data in Table 1.

<sup>c</sup>  $\text{III/Cis} = \text{IC}_{50}(\text{III})/\text{IC}_{50}(\text{Cisplatin})$ ,  $\text{III/Oxp} = \text{IC}_{50}(\text{III})/\text{IC}_{50}(\text{Oxaliplatin})$ . III/Cis and III/Oxp were calculated based on data in Ref. 19.

cytotoxicity against which was stronger than that of control drugs cisplatin and oxaliplatin. Moreover, the antitumor activities of ANOxp are remarkably more potent than its precursors O1 and A, as well as the mixture A&O1. Thereby, the conjugation of oxoplatin with naphthalimide acid to form ANOxp displays significant positive effects on antitumor activities.

Importantly, ANOxp exerts great potential in overcoming resistance of cisplatin. ANOxp reduces the resistant factor (RF) toward A549R to 0.5 from 1.7 for cisplatin, which is even more effective than oxaliplatin (RF = 0.8). However, ANOxp shows no obvious selectivity to tumor cells, and it displays  $\text{IC}_{50}$  value of  $6.4\text{ }\mu\text{M}$  toward normal cell 293 T, which is comparable to that of cisplatin and oxaliplatin.

To compare the antitumor activities of ANOxp with complex III, the ratio of their  $\text{IC}_{50}$  values to that of cisplatin and oxaliplatin were calculated respectively and provided in Table 2. Moreover, water solubility for both compounds was tested and the lipid-water partition coefficient Alog P was also calculated. As observed that ANOxp exhibits more potent activities than complex III *in vitro*, and the enhanced activities seem to relevant with the water solubility and lipid-water partition properties. The more potent mono aminonaphthalimide pended platinum(IV) ANOxp possesses a 4.0 times higher solubility than the dual substituted complex III in water, meanwhile ANOxp also displays satisfactory lipid-water distribution (2.713) in comparison with complex III (3.764). Accordingly, the design of mono aminonaphthalimide platinum(IV) complex ANOxp is proven a useful strategy in enhancing antitumor activities of platinum(IV) compounds.

To further confirm the antitumor competence of ANOxp, its activities *in vivo* were evaluated with oxaliplatin as reference drug. The BALB/c mouse bearing CT26 xenograft tumor was selected as model for the reason that the immune system is important for the anticancer activity of oxaliplatin and its derivatives.<sup>26,27</sup> Oxaliplatin and ANOxp were injected *via* intraperitoneal injection (i.p.) at days 6, 9, 12, 15 and 18 post-tumor inoculation with dosage of 5 mg Pt per kg, with saline as negative reference. The results in Fig. 3 show that ANOxp could effectively inhibit the growth of tumor in contrast to the NaCl group (Fig. 3A). Furthermore, the average tumor weight for ANOxp treated group at the end of the treatment is 0.17 g with tumor growth inhibition

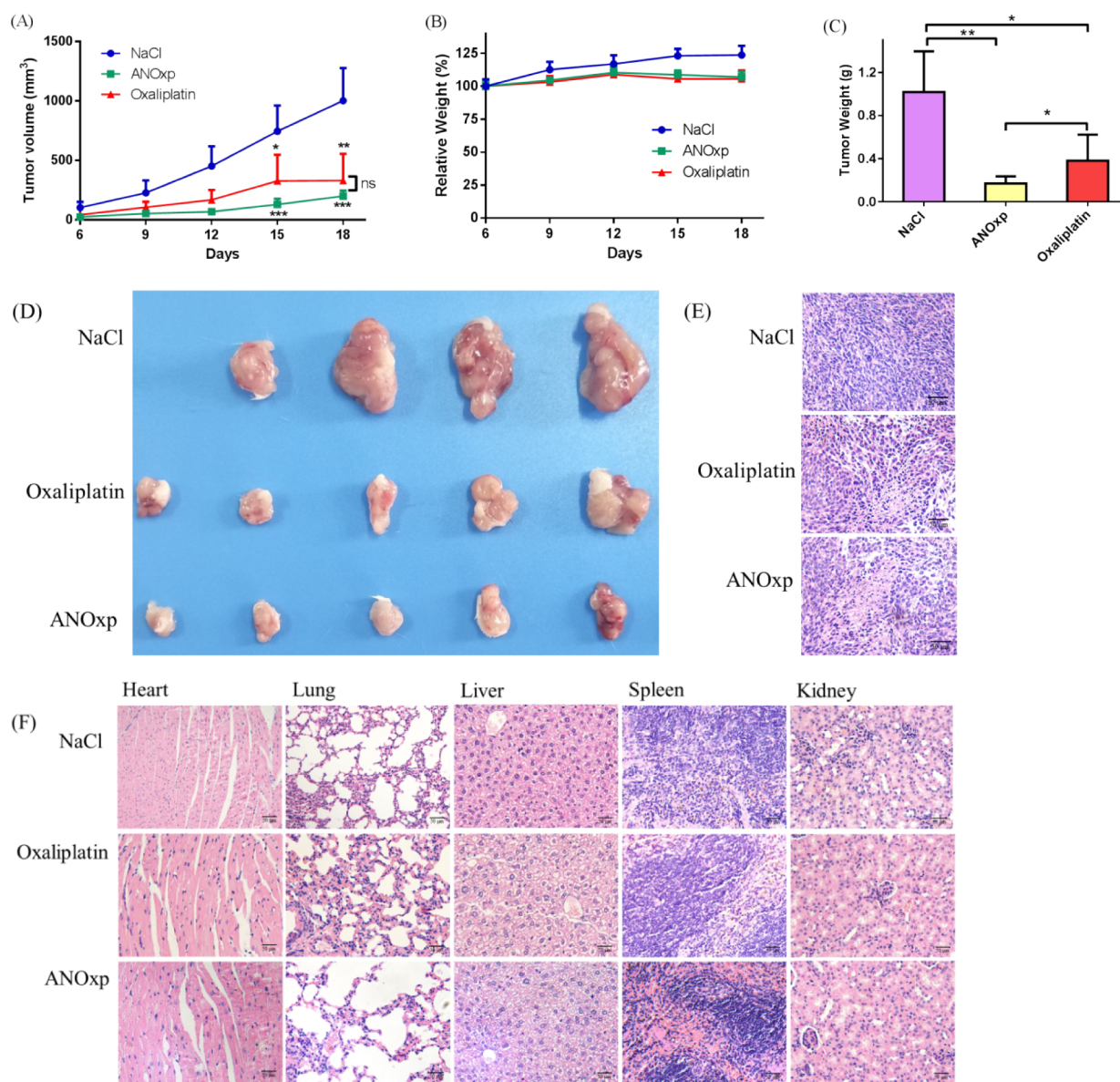


**Fig. 3.** *In vivo* antitumor activities of ANOxp and oxaliplatin against CT26 xenograft tumors in BALB/c mice. (A) Tumor growth as a function of time. (B) The body weight of the mice during the treatment. (C) The tumor weight in each group at the end of the experiment. (D) The images of the tumors at the end of the experiment. (E) Final magnification (200 ×) of the H&E staining of slices from tumor. (E) Final magnification (200 ×) of the H&E staining of slices from normal tissues. Results are representative of at least three independent experiments and shown as the mean ± S.D. \**p* < 0.05, \*\**p* < 0.01, \*\*\**p* < 0.001, ns: no significant difference compared with control group.

(TGI) of 83% compared to the NaCl group (1.02 g), which is more effective than the oxaliplatin group (0.38 g, 62%) (Fig. 3C and D). Then, the hematoxylin and eosin (H&E) staining slices from tumours in Fig. 3E manifest that ANOxp induces significant histological change to tumor tissues in contrast to the NaCl group, which is similar to that of oxaliplatin. The average tumor cell numbers in each microscopic field for the ANOxp treated group are less than the NaCl group, which demonstrates the inhibitory effects of ANOxp on proliferation of tumor cells. When consider the toxic effects of ANOxp, we find that ANOxp causes no remarkable body weight loss of the mice during such experiment progress (Fig. 3B). Moreover, no noticeable organ damages or appreciable histological differences of H&E staining slices from normal tissues including heart, lung, liver, spleen and kidney is found after treatment with ANOxp. These facts disclose that ANOxp displays no severe side effects on mice. Therefore, ANOxp could significantly inhibit the growth of CT-26 xenograft tumors *in vivo*, which are even better than oxaliplatin, without causing remarkable side effects.

ANOxp was supposed to display a dual DNA damage mechanism by the aminonaphthalimide and platinum groups. Its potential antitumor mechanism was investigated by electrophoretic dsDNA plasmid assay, fluorescence, UV-vis, CD and HPLC methods.

The electrophoretic dsDNA plasmid assay for DNA binding studies of ANOxp in Fig. 4 reveals that plasmid pAUR101 keeps stable for at least 4 h in PBS (bands a and b). Meanwhile, ANOxp effectively causes untwisting of the covalently closed circular plasmid within 4 h (bands e and f) which is similar to that of the platinum(II) reference drug oxaliplatin (bands c and d). These facts are probably owing to the intercalation of ANOxp with DNA plasmid *via* naphthalimide fragment. The platinum(IV) core is considered to release platinum(II) complex after reduction and realize the DNA damage function. Thus, the reduced system of ANOxp (ANOxp&AsA) was prepared under treatment of ascorbic acid (AsA) at 37 °C for 48 h to allow the platinum(IV) complex fully converting to divalent form. Bands g and h show that the reduced system ANOxp&AsA causes even much faster and more serious damage

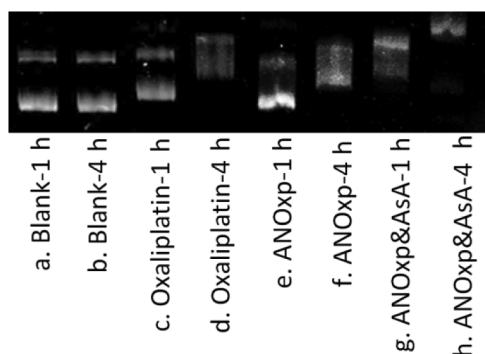


**Fig. 4.** Electropherograms of dsDNA plasmid pAUR101 incubated with 50  $\mu\text{M}$  of oxaliplatin, platinum(IV) compound ANOxp or its reduced system ANOxp&AsA for different incubation time (1 h or 4 h) at 37  $^{\circ}\text{C}$ .

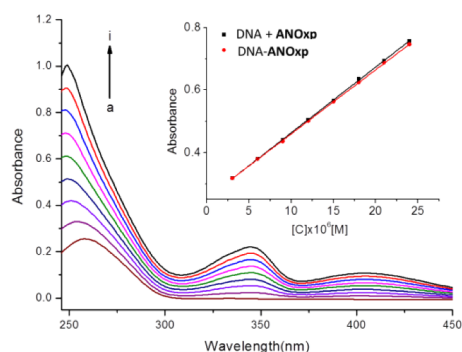


**Fig. 5.** UV-vis absorption spectra of CT-DNA (43.0  $\mu\text{M}$ ) in the absence and presence of compound ANOxp. a-i:  $c(\text{ANOxp}) = 0.0\text{--}24.0\ \mu\text{M}$  with increments of 3.0  $\mu\text{M}$ . Inset: The comparison of absorbance at 260 nm between the DNA-ANOxp system (DNA-ANOxp) and the sum values of free compound ANOxp and free DNA (DNA + ANOxp).

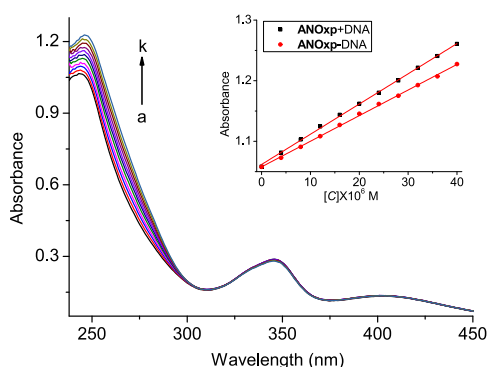


**Fig. 6.** UV-vis absorption spectra of ANOxp (40.0  $\mu\text{M}$ ) in the absence and presence of CT-DNA. a-i:  $c(\text{CT-DNA}) = 0.0\text{--}40.0\ \mu\text{M}$  with increments of 4.0  $\mu\text{M}$ . Inset: The comparison of absorbance at 250 nm between the ANOxp-DNA system (ANOxp-DNA) and the sum values of free compound ANOxp and free DNA (ANOxp + DNA).

to DNA than ANOxp and oxaliplatin, which are perhaps because of the synergetic function of the released platinum(II) complex and the naphthalimide moiety.

Then the UV-vis method was applied to detect the interaction of ANOxp with calf thymus-DNA (CT-DNA). UV-vis absorption spectra of CT-DNA in the absence and presence of ANOxp (Fig. 5) display that the absorption of CT-DNA at 260 nm increases gradually with the addition of ANOxp. Moreover, a hypochromic effect is observed that the absorption of DNA-ANOxp system is relatively weaker than the summation of ANOxp with DNA (DNA + ANOxp) (Inset of Fig. 5). Then, UV-vis absorption spectra of ANOxp in the absence and presence of CT-

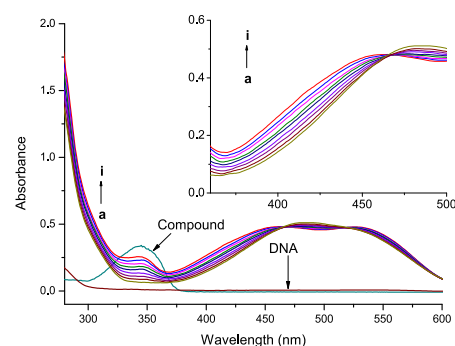


**Fig. 7.** UV-vis absorption spectra of NR-DNA system in the absence and presence of compound ANOxp (pH = 7.4,  $T = 298\ \text{K}$ ).  $c(\text{NR}) = 40.0\ \mu\text{M}$ ,  $c(\text{DNA}) = 43\ \mu\text{M}$ . a-k:  $c(\text{ANOxp}) = 0.0\text{--}30.0\ \mu\text{M}$  with increments of 3.0  $\mu\text{M}$ ; l: spectrum of ANOxp (30  $\mu\text{M}$ ); m: spectrum of CT-DNA (43  $\mu\text{M}$ ).

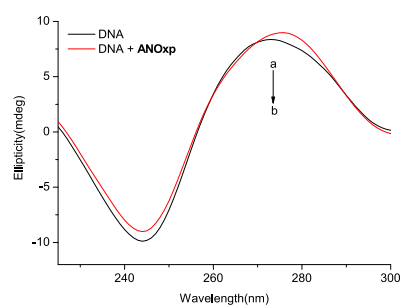


**Fig. 8.** CD spectra of CT-DNA in the absence and presence of the platinum(IV) compound ANOxp. a-b:  $c(\text{DNA}) = 80\ \mu\text{M}$ ,  $c(\text{ANOxp}) = 0, 20\ \mu\text{M}$ .

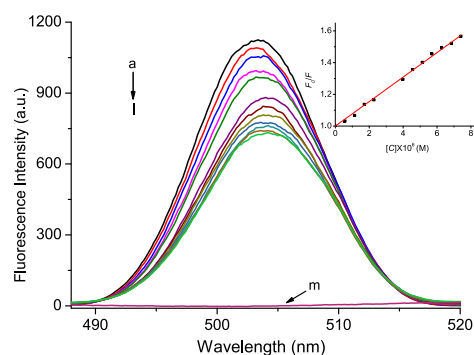


**Fig. 9.** Fluorescence spectrum of CT-DNA (100  $\mu\text{M}$ ) in the absence and presence of ANOxp ( $\lambda_{\text{ex}} = 260\ \text{nm}$ ,  $T = 298\ \text{K}$ ). a-l:  $c(\text{ANOxp}) = 0.00, 0.57, 1.14, 1.71, 2.28, 3.99, 4.56, 5.13, 5.70, 6.27, 6.84, 7.41\ \mu\text{M}$ ; m: spectrum of ANOxp (7.41  $\mu\text{M}$ ). Inset: Stern-Volmer plots for  $F_0/F$  vs.  $[C] \times 10^6$  of CT-DNA and ANOxp system.

DNA in Fig. 6 provides similar results. A hypochromic effect for ANOxp-DNA system was also revealed at 246 nm than ANOxp + DNA (Inset of Fig. 6). The facts mentioned above evidence the interaction of ANOxp with CT-DNA.

Neutral red (NR) was a planar phenazine dye which could interact with DNA by intercalated function. It is observed in Fig. S2 that CT-DNA could combine with NR to form a stable complex NR-DNA and further cause a decrease of the absorption peak for NR at 450 nm. Then, ANOxp was added to the NR-DNA system (Fig. 7). The absorption at 450 nm gradually increases with the concentration of ANOxp rising from 0.0  $\mu\text{M}$  to 24.0  $\mu\text{M}$ , which is probably ascribed to the competitive binding of ANOxp and NR with CT-DNA and further leading to the release of NR from the NR-DNA complex.

Further evidence for interaction of ANOxp with DNA was obtained by CD assay (Fig. 8), which is a sensitive optical technique in

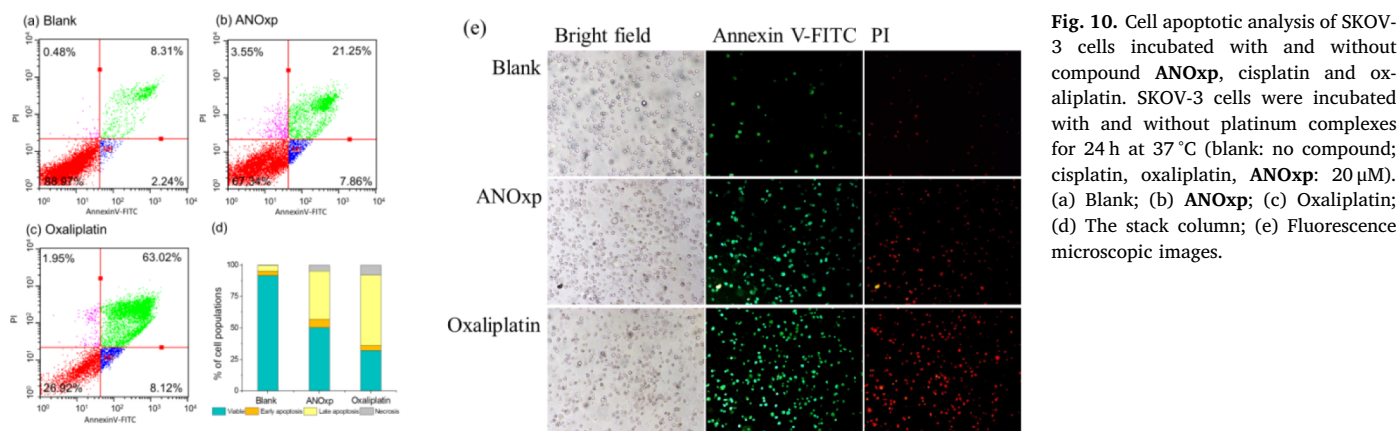


**Fig. 10.** Cell apoptotic analysis of SKOV-3 cells incubated with and without compound ANOxp, cisplatin and oxaliplatin. SKOV-3 cells were incubated with and without platinum complexes for 24 h at 37 °C (blank: no compound; cisplatin, oxaliplatin, ANOxp: 20  $\mu$ M). (a) Blank; (b) ANOxp; (c) Oxaliplatin; (d) The stack column; (e) Fluorescence microscopic images.

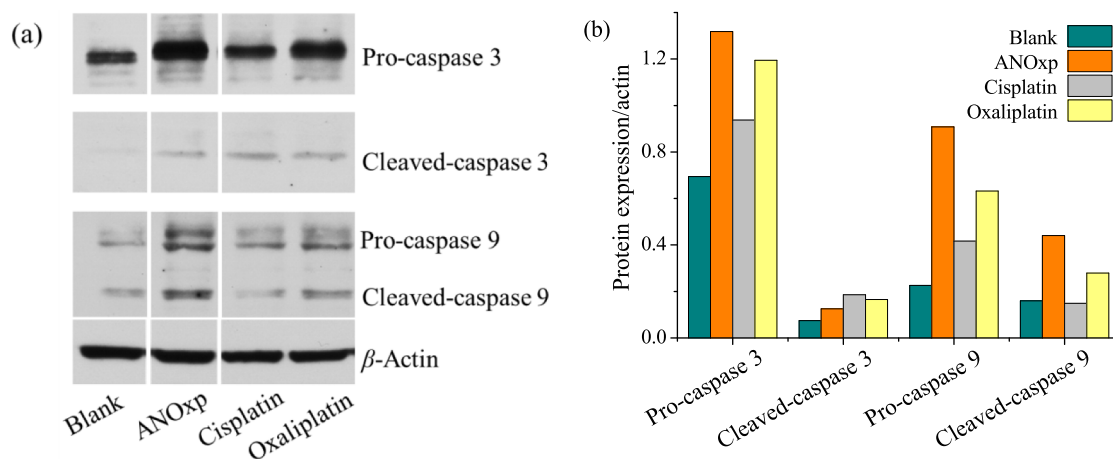


**Fig. 11.** Western blot analysis of cell apoptotic pathway induced by platinum complexes. SKOV-3 cells were incubated with and without compound ANOxp, cisplatin and oxaliplatin for 24 h at 37 °C (blank: untreated group; oxaliplatin, ANOxp: 30  $\mu$ M). (a) Blots; (b) Relative gray intensity analysis (Relative gray intensity = (gray intensity of indicated protein)/(gray intensity of  $\beta$ -actin)).

monitoring the structural change of DNA. The two typical peaks of CT-DNA (80.0  $\mu$ M) at 245 nm and 275 nm change simultaneously with the addition of ANOxp (20  $\mu$ M). The decrease of the negative peak at 245 nm manifests the reduction of right-handed helicity, meanwhile the increase of positive peak at 275 nm is attributed to the change of base stacking. These facts reflect the combination of ANOxp with CT-DNA.

The fluorescence spectrum was then utilized to further verify the interaction of ANOxp with DNA. The CT-DNA (100  $\mu$ M) displays typical fluorescence emission at 503 nm under excitation of 260 nm. ANOxp quenches the emission of CT-DNA gradually with the concentration rising to 7.41  $\mu$ M (Fig. 9). The quenching trend is in accordance with the Stern-Volmer equation. Then the Stern-Volmer constant  $K_{SV}$  ( $7.7 \times 10^4 \text{ M}^{-1}$ ) and quenching rate constant  $K_q$  ( $7.7 \times 10^{12} \text{ M}^{-1} \text{ s}^{-1}$ ) were calculated based on the Stern-Volmer equation (the detail calculation procedure was applied in ESI). Notably,  $K_q$  is greater than the maximum scatter collision quenching constant of the biomolecule ( $2.0 \times 10^{10} \text{ M}^{-1} \text{ s}^{-1}$ ) and this procedure is probably a static quenching on account of ANOxp interacting with the CT-DNA.

The reduction potential of platinum(IV) complexes to the divalent form, and the further DNA combination of the liberated platinum(II) complexes play key roles in the activation of platinum(IV) compounds. Herein, HPLC assay was employed to investigate the reduction and DNA damage abilities of ANOxp. The results in Fig. S3 indicate that ANOxp keeps stable for at least 8 h in PBS solution. It could easily undergo reduction in the presence of reducing AsA accompanied with the release of aminonaphthalimide acid. The formation of Platined-GMP peak proves the DNA interaction properties of the liberated platinum(II) complex. Summarily, platinum(IV) ANOxp easily undergoes reduction

in reducing condition. Then the released platinum(II) complex after reduction would effectively combine with DNA, and cause serious damage in tumor cells.

The apoptosis inducing properties were evaluated using annexin V-FITC and propidium iodide (PI) double-staining method and the expression of apoptosis proteins caspase 3 and caspase 9 were monitored by western blot assay. ANOxp effectively leads SKOV-3 cells undergo apoptosis (29.11%) in contrast to the blank group (10.55%) (Fig. 10). Furthermore, oxaliplatin (71.14%) seems more effective than ANOxp in inducing apoptosis. This is probably because of that the activation of platinum(IV) complex in tumor cells is accompanied with the reduction to divalent form, which costs longer time than platinum(II) drugs. Moreover, these results are reconfirmed by the following fluorescence microscopic images (Fig. 10e). Additionally, the western blot results in Fig. 11 display that the expression levels of pro-caspase 3 and pro-caspase 9 as well as the cleaved-caspase 3 and cleaved-caspase 9 increase conspicuously in ANOxp group in comparison with the blank group. Notably, ANOxp up-regulates the expression of proteins pro-caspase 3, pro-caspase 9 and cleaved-caspase 9 even more effectively than reference drugs cisplatin and oxaliplatin. Accordingly, ANOxp could induce cell apoptosis through an intrinsic apoptosis pathway.

In conclusion, a new aminonaphthalimide platinum(IV) complex ANOxp was designed, prepared and evaluated for antitumor activities *in vitro* and *in vivo*. The bioactivities *in vitro* reflects the effective activities of ANOxp to all the tested tumor cell lines, which are comparable or even better than reference drugs cisplatin and oxaliplatin. It exerts much potential in overcoming drug resistance of cisplatin. More importantly, ANOxp could effectively inhibit the growth of CT26

xenograft tumors in BALB/c mice without inducing severe side effects *in vivo*. Furthermore, a dual DNA damage mechanism is evidenced by multiple strategies that ANOxp could interact with DNA in tetravalent form *via* the naphthalimide ligand and cause DNA lesion. Further reduction to platinum(II) complex would induce remarkable secondary damage to DNA. Moreover, ANOxp effectively cause apoptosis of tumor cells by up-regulating the expressions of caspase 3 and caspase 9. These findings enable ANOxp to be a prominent compound for further investigation as new anticancer agents.

#### Declaration of Competing Interest

The authors declare that they have no known competing financial interests or personal relationships that could have appeared to influence the work reported in this paper.

#### Acknowledgements

The work was supported by National Natural Science Foundation of China (No. 21807056), Natural Science Foundation of Shandong, China (No. ZR2017BH092), Doctoral Foundation of Liaocheng University, China (No. 318051635), Open Project of Shandong Collaborative Innovation Center for Antibody Drugs (No. CIC-AD1836, CIC-AD1835), National Science and Technology Major Project of China (No. 2017ZX09201-003) and Taishan Scholar Research Foundation. This work was also technically supported by Shandong Collaborative Innovation Center for Antibody Drugs and Engineering Research Center for Nanomedicine and Drug Delivery Systems.

#### Appendix A. Supplementary data

Supplementary data to this article can be found online at <https://doi.org/10.1016/j.bmcl.2019.126670>.

#### References

1. Wong E, Christen MG. *Chem Rev.* 1999;99:2451.
2. Allardyce CS, Dyson PJ. *Dalton Trans.* 2016;45:3201.
3. Arambula JF, Sessler JL, Siddik ZH. *Bioorg Med Chem Lett.* 2011;21:1701.
4. Oun R, Mouss YE, Wheate NJ. *Dalton Trans.* 2018;47:6645.
5. Facchetti G, Rimoldi I. *Bioorg Med Chem Lett.* 2019;29:1257.
6. Yang M, Pang RF, Jia X, Wang K. *J Inorg Biochem.* 2005;99:376.
7. Gao C, Gou S, Fang L, Zhao J. *Bioorg Med Chem Lett.* 2011;21:1763.
8. Tan XX, Li GS, Wang QP, Wang BQ, Li DC, Wang PG. *Prog Chem.* 2018;30:831.
9. Gibson D. *Dalton Trans.* 2016;45:12983.
10. Johnstone TC, Suntharalingam K, Lippard SJ. *Chem Rev.* 2016;116:3436.
11. Schreiber-Brynzak E, Pichler V, Heffeter P, et al. *Metallomics.* 2016;8:422.
12. Wexselblatt E, Gibson D. *J Inorg Biochem.* 2012;117:220.
13. Song Y, Suntharalingam K, Yeung JS, Royzen M, Lippard SJ. *J Inorg Biochem.* 2013;24:1733.
14. Kenny RG, Su WC, Crawford A, Marmion CJ. *Eur J Inorg Chem.* 2017;12:1596.
15. Basu U, Banik B, Wen R, Pathak RK, Dhar S. *Dalton Trans.* 2016;45:12992.
16. Gabano E, Ravera M, Osella D. *Dalton Trans.* 2014;43:9813.
17. Qin X, Fang L, Chen F, Gou S. *Eur J Med Chem.* 2017;137:167.
18. Wang Z, Xu Z, Zhu G. *Angew Chem.* 2016;55:15564.
19. Wang QP, Tan XX, Liu ZF, et al. *Eur J Pharm Sci.* 2018;124:127.
20. Wang QP, Li GS, Liu ZF, et al. *Eur J Inorg Chem.* 2018;40:4442.
21. Ma J, Wang Q, Huang Z, et al. *J Med Chem.* 2017;60:5736.
22. Li GS, Zhang JF, Liu ZF, et al. *J Inorg Biochem.* 2019;194:34.
23. Wang QP, Chen Y, Li GS, et al. *Bioorg Med Chem.* 2019;27:2112.
24. Wang QP, Huang ZL, Ma J, et al. *Dalton Trans.* 2016;45:10366.
25. Wheate NJ, Walker S, Craig GE, Oun R. *Dalton Trans.* 2010;39:8113.
26. Göschl S, Schreiber-Brynzak E, Pichler V, et al. *Metallomics.* 2017;9:309.
27. Jungwirth U, Xanthos DN, Gojo J, et al. *Mol Pharmacol.* 2012;81:719.